

Anderson Localization in Euclidean Random Matrices

S. Ciliberti,^{1,2} T. S. Grigera,³ V. Martín-Mayor,^{1,2} G. Parisi,⁴ and P. Verrocchio^{1,2}

¹*Departamento de Física Teórica I, Universidad Complutense de Madrid, Madrid 28040, Spain*

²*Instituto de Biocomputación y Física de Sistemas Complejos (BIFI). Universidad de Zaragoza, 50009 Zaragoza, Spain.*

³*Instituto de Investigaciones Fisicoquímicas Teóricas y Aplicadas (INIFTA), c.c. 16, suc. 4, 1900 La Plata, Argentina.*

⁴*Dipartimento di Fisica, Università di Roma "La Sapienza", INFN unità di Roma I, and Center for Statistical Mechanics and Complexity (SMC), P.le A. Moro 2, I-00185 Roma, Italy*

We study spectra and localization properties of Euclidean random matrices. The problem is approximately mapped onto that of a matrix defined on a random graph. We introduce a powerful method to find the density of states and the localization threshold. We solve numerically an exact equation for the probability distribution function of the diagonal element of the the resolvent matrix, with a population dynamics algorithm, and we show how this can be used to find the localization threshold. An application of the method in the context of the Instantaneous Normal Modes of a liquid system is given.

PACS numbers: PACS

Introduction. Some forty years ago Anderson [1] pointed out that disorder can turn a system expected to be a metal from band-theory (i.e. a gapless system) into an electric insulator. This gave birth to the difficult problem of Anderson localization [2, 3, 4, 5]. The physical picture is roughly the following: In a pure system, states are described by Bloch wavefunctions. Disorder divides the energy band in localized (wavefunctions extending over a limited number of unit cells) and extended regions (wavefunctions are plane-wave like, involving an extensive number of lattice sites). The energy marking this division is called *mobility edge* or localization threshold. If the Fermi level lies in the localized region, transport is strongly hampered. Given the large variety of systems that are described to some degree of approximation by random matrices [6], it has become clear that Anderson localization is significant beyond the physics of disordered metals. However, there are very few situations [3, 7] where it is possible to estimate the position of the mobility edge in a controlled manner, and often heuristic estimates are used (some authors identify it with the Ioffe-Regel limit or with the limits of the spectrum obtained in some kind of effective-medium approximation [8]), or numerical evaluations based on a variety of ideas (see e.g. refs. 9 or 10). In this Letter we present a method to locate the mobility edge for Euclidean Random Matrices [11] (ERM), which we illustrate in a liquid calculation of Instantaneous Normal Modes [12] (INM).

The entries of an ERM are deterministic functions of (random) particle positions. Conservation laws (see below) are encoded in the constraint that the sum of all elements in a row is null. ERMs appear in the study of disordered d -wave superconductors [13], disordered magnetic semiconductors [14] (very similar to a spin-glass model [15]), INM in liquids [16, 17], vibrations in glasses [18], the gelation transition in polymers [19] and vibrations in DNA [20]. Also, theoretical studies have been carried out [21].

ERMs in liquids. Consider a translationally invariant system with Hamiltonian $H[\vec{x}] = \sum_{i<j} v(\vec{x}_i - \vec{x}_j)$, for some pair potential $v(\vec{x})$. The system has N particles in a box of volume V , the particle density being $\rho = N/V$. We impose a long-distance cut-off on $v(\vec{x})$, as usual in numerical simulations. In studies of short-time dynamics [12] the harmonic approximation is made around the oscillation centers \vec{x}^c . We thus face the Hessian matrix $M_{i\mu,j\nu}[\vec{x}^c] \equiv -v_{\mu\nu}(\vec{x}_i^c - \vec{x}_j^c) + \delta_{ij} \sum_{k=1}^N v_{\mu\nu}(\vec{x}_i^c - \vec{x}_k^c)$, where $v_{\mu\nu}(\vec{x})$ is the second derivative matrix of $v(\vec{x})$. As it should, the sum of all elements in a matrix row is zero. Once the probability density function (pdf) of the oscillation centers, $P[\vec{x}^c]$, is specified, the study of the spectral properties of the Hessian is a problem on ERM theory [11]. In the context of supercooled liquids, people have considered three types of $P[\vec{x}^c]$: equilibrium configurations [12] (the INM), minima [22] and saddle-points [23] of the potential energy surface. As in all previous analytical studies, we restrict ourselves to INM.

The resolvent and its equation. We need to consider the resolvent matrix [2], $R_{i\mu,j\nu}(z) = (z - M)_{i\mu,j\nu}^{-1}$ (z is complex). To study eigenvalues clustered around λ , we will set $z = \lambda + i\varepsilon$ for small ε . Our goal is to find an equation for the pdf of the diagonal term of the resolvent matrix [26], $\mathcal{P}[\mathbf{R}_{ii}(z)]$, focusing its imaginary part. Consider the representation of $\mathbf{R}_{ii}(z)$ in terms of the eigenvectors $|\alpha\rangle$ of the matrix M :

$$\text{Im } R_{jj}(\lambda + i\varepsilon) = \text{Im} \sum_{\alpha} \frac{|\langle j|\alpha\rangle|^2}{\lambda + i\varepsilon - \lambda_{\alpha}}. \quad (1)$$

Previous calculations [8, 16, 17] only addressed the *mean value* of $\mathcal{P}[\mathbf{R}_{ii}(z)]$, which gives the density of states (DOS) through $g(\lambda) = -\frac{1}{3N\pi} \text{Im} \overline{\sum_i \text{Tr} \mathbf{R}_{ii}(\lambda + i0^+)}$ (the overline indicates mean value). Localization studies [2] require at least the variance of $\mathcal{P}[\mathbf{R}_{ii}(z)]$, as can be seen from Eq. 1: Consider a λ in the localized region. The amplitude of eigenvectors $|\alpha\rangle$ with $|\lambda_{\alpha} - \lambda| \lesssim \varepsilon$ will be large for the main particle of the eigenmode, and will de-

crease exponentially with the distance. Let $n(\lambda)$ be the typical number of particles for which the amplitude of an eigenmode is sizeable. The probability that in Eq. 1 particle j will significantly participate in an eigenvector of energy $\lambda_\alpha \in (\lambda - \varepsilon, \lambda + \varepsilon)$ is of order $\varepsilon g(\lambda) n(\lambda)$. In this case $\text{Im } R_{jj}$ is of the order $1/(\varepsilon n(\lambda))$, while it is of order ε with probability $1 - \varepsilon g(\lambda) n(\lambda)$. Thus, the mean value of $\text{Im } R_{jj}$ is finite for small ε and proportional to $g(\lambda)$, but its variance is $\sigma^2(\lambda; \varepsilon) \simeq g(\lambda)/(\varepsilon n(\lambda))$ and it diverges for vanishing ε . A more refined analysis [3] shows that the pdf for $\text{Im } R_{jj}$ decays as $(\text{Im } R_{jj})^{-\beta}$, $\beta \leq 1.5$, with an unknown cutoff function that prevents $\text{Im } R_{jj} > 1/\varepsilon$. On the other hand, in the extended region, all the $|\langle j|\alpha \rangle|^2$ are $\mathcal{O}(1/N)$ and one can replace the sum with an integral. It follows that the typical value of $\text{Im } R_{jj}$ is a number of order one when $\varepsilon = 0^+$.

To get an equation for $\mathcal{P}[\mathbf{R}_{ii}(z)]$, we have considered the generalization of the Cizeau-Bouchaud recursion relation [7] to the case of translationally invariant systems [25]. This equation relates $\mathbf{R}_{ii}(z)$ in a system with N particles to the *full* resolvent of a system where particle i is not present anymore, but the positions of all other $N - 1$ particles are as in the original system. To use that equation we need to make a rather drastic simplification regarding particle correlations: following ref. 16, we regard the matrix elements $M_{i\mu, j\nu}[\mathbf{x}^c]$ as independent random variables, $\mathbf{P}[\mathbf{M}] = \prod_{i < j} \mathbf{p}(\mathbf{M}_{ij})$. Thus we throw away most of the information contained in the Boltzmann weight $P[\mathbf{x}^c]$, restricting ourselves to the pair correlation function $g^{(2)}(r)$. Therefore, $\mathbf{p}(\mathbf{M}_{ij})$ is the pdf of the single matrix element,

$$\mathbf{p}(\mathbf{M}_{ij}) = \left(1 - \frac{\gamma}{N}\right) \delta(\mathbf{M}_{ij}) + \frac{\rho}{N} \int_0^{r^{\text{cut}}} d\vec{r} g^{(2)}(r) \delta(\mathbf{M}_{ij} + \mathbf{v}''(\vec{r})), \quad (2)$$

where $\gamma = 4\pi\rho \int_0^{r^{\text{cut}}} dr' r'^2 g^{(2)}(r')$ [27] is the average number of particles whose distance from particle i is less than the cut-off. In other words, we have considered the problem on a random graph [24, 25]: each particle is the root of a Cayley tree whose fluctuating connectivity is distributed with a Poisson law of mean value γ . Under these hypothesis the central equation of this Letter is obtained [25]:

$$\mathcal{P}[\mathbf{R}_{ii}(z)] = \int d\mathbf{P}[\mathbf{M}] d\mathcal{P}[\mathbf{R}_{jj}] \delta \left[\mathbf{R}_{ii} - \left(z + \sum_{j \neq i} \mathbf{M}_{i,j} - \sum_{j \neq i} \mathbf{M}_{ij} (\mathbf{R}_{jj}^{-1} + \mathbf{M}_{ij})^{-1} \mathbf{M}_{ji} \right)^{-1} \right]. \quad (3)$$

Here the inverse-matrix symbols refer to the 3×3 dimensional space of the directions for particle displacements. Note also that all the \mathbf{R}_{jj}^{-1} are independently chosen from the $\mathcal{P}[\mathbf{R}_{jj}(z)]$ distribution.

Solving the equation. We shall consider the case of the INM of a monoatomic system with potential (in natural units) $v(r) = (1/r)^{12}$, with a smooth cutoff at $r^{\text{cut}} = 15\sqrt{3}/13$ (see Grigera *et al.* in [23] for details). As the only relevant thermodynamic parameter is $\Gamma = \rho T^{-1/4}$, we shall take $\rho = 1$. We have obtained the pair correlation function by means of a Monte Carlo simulation of an $N = 2048$ system, for Γ between 0.3 and 1.1, in the liquid phase (crystalization happens at $\Gamma_c \approx 1.14$). We have also obtained the INM spectrum numerically (diagonalizing 100 Hessian matrices), in order to assess the quality of our approximations for particle correlations. Once the $g^{(2)}(r')$ is known, one needs to solve Eq. (3). We have done this numerically, by means of a population dynamics algorithm (PDA). Starting from a population of N elements with $\mathbf{R}_{ii}(z; t = 0) = \mathbf{I}/z$, we iterate the scheme

$$\mathbf{R}_{ii}(z; t + 1) = \mathbf{F}(\mathbf{R}_{jj}(z; t), \mathbf{M}_{ij}), \quad (4)$$

$$\mathbf{F}(\mathbf{R}_{jj}, \mathbf{M}_{ij}) \equiv \left[z\mathbf{I} + \sum_j \mathbf{M}_{ij} - \sum_{j \neq i} \mathbf{M}_{ij} (\mathbf{R}_{jj}^{-1} + \mathbf{M}_{ij})^{-1} \mathbf{M}_{ji} \right]^{-1}. \quad (5)$$

To form the sums in (5), we divide the space around particle i up to the cutoff distance, in spherical shells of width $\Delta r = r^c/4096$. The probability of having a particle in the shell is $4\pi\rho \int_r^{r+\Delta r} dr' r'^2 g^{(2)}(r')$. Both the identity, j , of the particle interacting with particle i , and the direction of the vector $\vec{r} \equiv \vec{r}_i - \vec{r}_j$ are chosen randomly with uniform probability. A single time-step consists on the sequential update of the full population. We equilibrate for 100 time steps, which is verified to be enough by checking the time evolution of the first moments of the distribution. We then evaluate $\mathcal{P}[\mathbf{R}_{ii}(z)]$ by means of (typically) 300 population-dynamics time steps. The population averages of $\text{Im } R_{i\mu, i\mu}$ and $(\text{Im } R_{i\mu, i\mu})^2$ are calculated, then time-averaged. From them we compute the DOS, $g(\lambda) = -\text{Im } R_{i\mu, i\mu}/\pi$, and $\text{Im } R_{i\mu, i\mu}^2$. An important test is to compare the DOS obtained from Eq. 3 with the DOS obtained by numerical diagonalization of the scrambled matrix $\tilde{\mathbf{M}}$, built by picking its off-diagonal elements randomly and without repetition from the off-diagonal elements of the true Hessian, and then imposing the constraints of symmetry and translational invariance. This kills three-body and higher correlations, making Eq. 3 exact. In Fig. 1 we show the DOS at $\Gamma = 0.6$ and 1.1, computed both from Eq. 3 and from the numerical diagonalization of the Hessian. At $\Gamma = 0.6$ good agreement is found. At $\Gamma = 1.1$ we also show the DOS of the scrambled Hessian, which agrees with Eq. 3. One can understand the mild disagreement between Eq. 3 and the INM spectrum at $\Gamma = 1.1$ by comparing the pdf of the diagonal term of the Hessian matrix as computed from Eq. 2 and from the actual liquid configurations (Fig. 1). This pdf coincides with the DOS at the leading order in pertur-

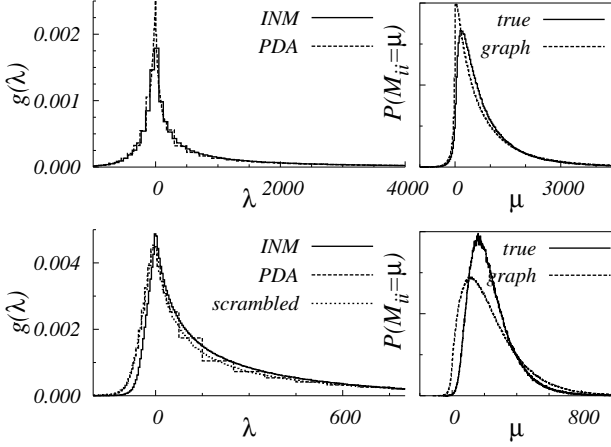


FIG. 1: **Top.** Left panel: DOS of a soft-sphere system at $\Gamma = 0.6$ from the solution of Eq. 3 for $\varepsilon = 1.0$ ($N = 20000$) and from the numerical diagonalization of the Hessian matrix. Right panel: distribution of the diagonal terms of the Hessian matrix, from Eq. 2 and from liquid simulations at $\Gamma = 0.6$. **Bottom:** As in the top part, for $\Gamma = 1.1$. The spectrum of the corresponding scrambled matrix (see text) is also shown.

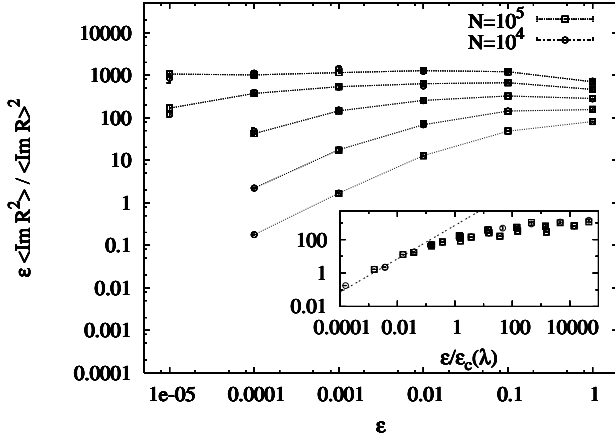


FIG. 2: $l(\lambda; \varepsilon)$ vs. ε near the lower mobility edge at $\Gamma = 1.1$ for (from top to bottom) $\lambda = -140, -130, -120, -110$, and -100 . Inset: Scaling plot $l(\lambda; \varepsilon)$ vs. $\varepsilon/\varepsilon_c(\lambda)$ for $\lambda \geq -130$.

bation theory (the diagonal term, \mathbf{M}_{ii} , is much larger than the typical off-diagonal term \mathbf{M}_{ij}), so we understand why at $\Gamma = 1.1$, Eq. 3 overestimates the weight of the imaginary frequencies.

Localization. In principle, one can establish the localization threshold from the behavior of the variance of the imaginary part of R . Consider $l(\lambda; \varepsilon) \equiv \varepsilon \langle \text{Im} R^2 \rangle / \langle \text{Im} R \rangle^2$. From the remarks above it follows that in the localized region and for small ε , $l(\lambda; \varepsilon)$ tends to a constant, while in the extended region the variance is finite and $l(\lambda; \varepsilon)$ is $\mathcal{O}(\varepsilon)$. Fig. 2 shows $l(\lambda; \varepsilon)$ around the lower mobility edge. For the higher values of λ , the extended, $\mathcal{O}(\varepsilon)$ regime is reached, but as the threshold is

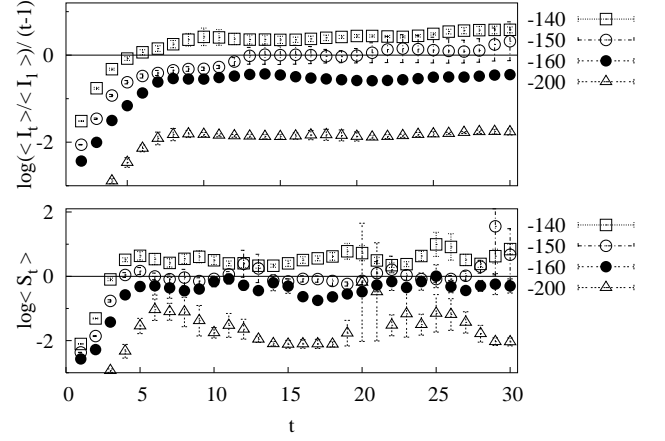


FIG. 3: Evolution of the median (top) and geometrical average (bottom) of the population of imaginary parts of the resolvent (see text) for $\lambda = -140, -150, -160$, and -200 . Data for $N = 10^6$.

approached, the regime sets in for lower and lower values of ε , making the threshold difficult to estimate. To overcome this limitation, we have tried the phenomenological scaling $l(\lambda, \varepsilon) = f(\varepsilon/\varepsilon_c(\lambda))$, with $f(x) \sim x$ for $x \sim 0$ and $\varepsilon_c(\lambda) \rightarrow 0$ for $\lambda \rightarrow \lambda_{\text{th}}$ (Fig. 2). The $\varepsilon_c(\lambda)$ (that we obtained only for $\lambda \geq -130$) can be fitted to a power law $c(\lambda - \lambda_{\text{th}})^\gamma$, with $\gamma = 21$ and $\lambda_{\text{th}} = -171.6$. This huge exponent is perhaps an indication of an essential singularity at the mobility edge (cf. the analytical results of ref. 5).

However, the fit is not very reliable, since it does not reach close enough to the critical point (moving nearer requires lowering ε , but this is computationally expensive since the statistics must grow as $1/\sqrt{\varepsilon}$ when the variance is growing as $1/\varepsilon$).

In search of a more reliable way to determine the threshold, we have tried a different method, based on the observation that in the localized region and in the $\varepsilon \rightarrow 0$ limit, $\text{Im} \mathbf{R}_{ii} = 0$ except for a vanishing fraction of particles, suggesting that a population of real resolvents is dynamically stable under Eq. 5. The idea [3] is to start with an equilibrated population of real resolvents (setting $z = \lambda$), add a small imaginary part and evolve the population with eq. 5 to see whether the imaginary parts grow (extended phase) or tend to disappear (localized phase). We have analyzed in this way the negative mobility edge at $\Gamma = 1.1$: We obtained an equilibrated population of real resolvents, then added an infinitesimal imaginary part, which evolved with the linearized (with respect to the imaginary part) form of Eq. 5. We evolved the real part with Eq. 5 as if the population were real. Since the pdf of $\text{Im} \mathbf{R}_{jj}^{(t)}$ is extremely broad, one must be careful in the quantity one chooses to examine. In ref. 3 it was proposed to consider the quotient S_t of the geometric mean of the imaginary parts at times t and

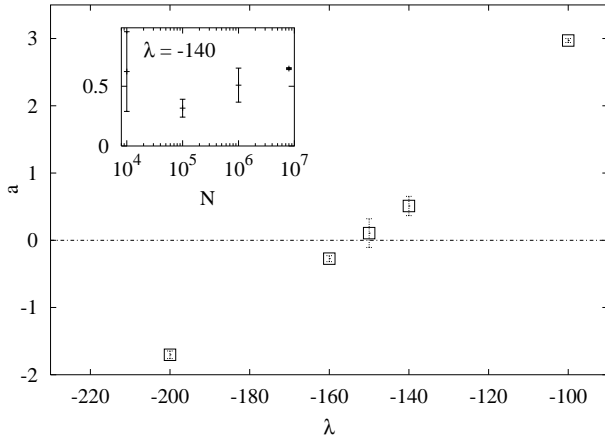


FIG. 4: Values of the slope from a linear fit of $\langle \log I_t \rangle$ for $t > 10$. The mobility edge is estimated at $\lambda = -152(5)$. Inset: N -dependence of the slope.

$t - 1$. S_t was assumed to be t -independent, and it was expected to be equal to 1 at the mobility edge. However, the threshold found with this method was far from theoretical estimates. Indeed, as can be seen in Fig. 3, this quantity has extremely large fluctuations, that make it practically useless to determine the threshold. Instead, we have found that the *median* (let us call it I_t) of the pdf of $\text{Im } \mathbf{R}_{ii}^{(t)}$ is much more reliable. However, obtaining the thermodynamic limit for I_t requires N that grows fastly with t . For $t < 15$ we have found no differences between $N = 10^6$ and $N = 8 \times 10^6$. One would expect that $\log I_t \sim at$, with a less than (greater than) zero in the localized (extended) phase, and this is indeed what we find at large t (Fig. 3). For $N = 10^6$ we have performed 10 trajectories, then estimated the errors with a jackknife method. A linear fit of $\log I_t$, for $1 \leq t \leq 15$ gives values a that locate the mobility edge at $\lambda = -152(5)$ (Fig. 4).

In summary, we have addressed the problem of Anderson localization in Euclidean Random Matrices, specializing to a liquid Instantaneous Normal Modes calculation. Under the random-graph approximation for particle correlations, which keeps only the information of the radial distribution function, a closed equation was found for the pdf of the diagonal element of the resolvent matrix \mathbf{R}_{ii} . This equation was solved numerically by means of a population dynamics algorithm. We have shown that the random-graph approximation works rather well at low density, but significantly overestimates the weight of unstable modes when the system is close to crystallization. We have shown how to locate the mobility edge from the mean of the square of the imaginary part of $\mathbf{R}_{ii}(z)$. We have studied numerically the stability of a population of real resolvents, improving over the numerical method of Abou-Chacra *et al.* [3], and obtaining an estimate in rea-

sonable agreement with the value obtained with complex resolvents.

We acknowledge partial support from MCyT (Spain), contracts FPA2001-1813, FPA2000-0956 and BFM2003-08532-C03 and ANPCyT (Argentina). S.C. was supported by the ECHP programme under contract HPRN-CT-2002-00307, *DYGLAGEMEM*. T.S.G. is career scientist of CONICET (Argentina). V.M.-M. is a *Ramón y Cajal* research fellow. P.V. was supported by the European Commission through contract MCFI-2002-01262.

-
- [1] P. W. Anderson, Phys. Rev. **109**, 1492 (1958).
 - [2] J. T. Edwards, D. J. Thouless, J. Phys. C **5**, 807 (1972); D. J. Thouless, Phys. Rep. **13**, 93 (1974).
 - [3] R. Abou-Chacra *et al.*, J. Phys. C **6**, 1734 (1973).
 - [4] P. A. Lee, T. V. Ramakrishnan, Rev. Mod. Phys. **57**, 287 (1985).
 - [5] Y.V. Fyodorov *et al.*, J. Phys. (Paris) **I2**, 1571 (1992).
 - [6] M. L. Mehta, *Random Matrices* (Academic Press, New York, 1991).
 - [7] P. Cizeau, J. P. Bouchaud, Phys. Rev. E **50**, 1810 (1994).
 - [8] G. Biroli, R. Monasson, J. Phys. A: Math. Gen. **32**, L255 (1999); R. Monasson, Eur. Phys. J. B **12**, 555 (1999).
 - [9] P. Carpena, P. Bernaola-Galván, Phys. Rev. B **60**, 201 (1999); J. Fabian, Phys. Rev. B **55**, 3328 (1997); S. Bembenek, B. Laird, Phys. Rev. Lett. **74**, 936 (1995).
 - [10] B. Kramer, A. MacKinnon, Rep. Prog. Phys. **56**, 1469 (1993).
 - [11] M. Mézard *et al.*, Nucl. Phys. B **559**, 689 (1999).
 - [12] T. Keyes, J. Chem. Phys. **101**, 5081 (1994).
 - [13] C. Chamon, C. Mudry, Phys. Rev. B **63**, 100503(R) (2001).
 - [14] L. Brey, G. Gómez-Santos, Phys. Rev. B **68**, 115206 (2003).
 - [15] D. Dean, D. Lancaster, Phys. Rev. Lett. **77**, 3037 (1996).
 - [16] A. Cavagna *et al.*, Phys. Rev. Lett. **83**, 108 (1999).
 - [17] T. M. Wu, R. F. Loring, J. Chem. Phys. **97**, 8568 (1992); Y. Wan, R. Stratt, J. Chem. Phys. **100**, 5123 (1994).
 - [18] S. Ciliberti *et al.*, J. Chem. Phys. **119**, 8577 (2003); T. S. Grigera *et al.*, Phys. Rev. Lett. **87**, 85502 (2001).
 - [19] K. Broderix *et al.*, Phys. Rev. E **64**, 021404 (2001).
 - [20] S. Cocco, R. Monasson, Phys. Rev. Lett. **83**, 5178 (1999).
 - [21] E. Bogomonly *et al.*, J. Phys. A: Math. Gen. **36**, 3595 (2003); C. R. Offer, B. D. Simons, J. Phys. A: Math. Gen. **33**, 7567 (2000); A. Zee, I. Affleck, J. Phys.: Cond. Matter **12**, 8863 (2000); D.S. Dean, J. Phys. A: Math. Gen. **35**, L153 (2002).
 - [22] F.H. Stillinger, T. A. Weber, Science **225**, 983 (1984).
 - [23] L. Angelani *et al.*, Phys. Rev. Lett. **85**, 5356 (2000); K. Broderix *et al.*, Phys. Rev. Lett. **85**, 5360 (2000); T.S. Grigera *et al.*, Phys. Rev. Lett. **88**, 055502 (2002); D.J. Wales, J.P.K. Doye, *cond-mat/0309059*.
 - [24] A. J. Bray, G. J. Rodgers, Phys. Rev. B **38**, 11461 (1988).
 - [25] S. Ciliberti, Ph. D. Thesis (Università di Roma *La Sapienza*, 2003); S. Ciliberti *et al.*, in preparation.
 - [26] Boldface symbols represent 3×3 matrices corresponding to particle displacements in 3-D.
 - [27] In the case considered here, $\gamma \approx 32$, thus the probability of finding disconnected clusters is negligible [24].